Journal of Physics: Conference Series **88** (2007) 012034 doi:10.1088/1742-6596/88/1/012034

Photoelectron spectroscopy of the structure and dynamics of free size selected sodium clusters

Oleg Kostko, Christof Bartels, Jörg Schwöbel, Christian Hock, and Bernd v. Issendorff

Fakultät für Physik, Universität Freiburg, Hermann-Herder-Straße 3, 79104 Freiburg, Germany

E-mail: bernd.von.issendorff@uni-freiburg.de

Abstract. Photoelectron spectroscopy on free cold size-selected sodium clusters has led to a detailed knowledge of their electronic and geometric structures in a very broad size range. Even more information about the electronic structure of the clusters has been obtained now by angle resolved photoelectron spectroscopy, which in principle allows one to gain information about the character of the electronic wavefunctions. The results demonstrate that sodium clusters have an electronic structure close to that of an finite size free electron gas, which makes them perfect model systems for the study of many particle dynamics. One such measurement is the time-resolved study of the cooling of the hot electron gas in the cluster, which allowed to determine the size dependence of the electron phonon coupling strength.

1. Introduction

Bulk sodium is the best representative of a free electron metal[1, 2]. It can therefore be expected that sodium clusters have a very simple electronic structure. Indeed Knight et al. have demonstrated already in 1984 that the stability of sodium clusters is dominated by electron shell effects[3]. These shells are the consequence of the free nature of the electrons; the wave functions of the electrons in the (close to) spherical clusters are the angular momentum eigenstates, which can be additionally characterized by a radial quantum number. Clusters sizes for which all degenerate sublevels of a shell are filled are especially stable; for sodium these are the sizes 8 (filling of 1p), 20 (2s), 40 (2p), 58 (1g), 92 (1h), and so on. Electron shell effects in sodium clusters and other simple metal clusters have, apart from the mass spectroscopy studies, been seen in measurements of ionization potentials, absorption cross sections, polarizabilities and others[4, 5, 6]. But a direct observation of the electron shell structure in sodium clusters by photoelectron spectroscopy was only achieved recently[7]. This spectroscopy technique turned out to yield the most detailed information about the electronic and geometric structure of the clusters as well as ultrafast dynamics in the clusters. In this report the most important findings will be summarized. It is organized as follows: in the first part the experiment will be described; then experimental results of "normal" energy resolved photoelectron spectroscopy will be discussed, followed by a presentation of the very first results of angle resolved photoelectron spectroscopy obtained on free simple metal clusters. After this some results of pump-probe photoelectron spectroscopy will be presented, namely the determination of the electron-phonon coupling strength in sodium clusters, and last ongoing projects are described.

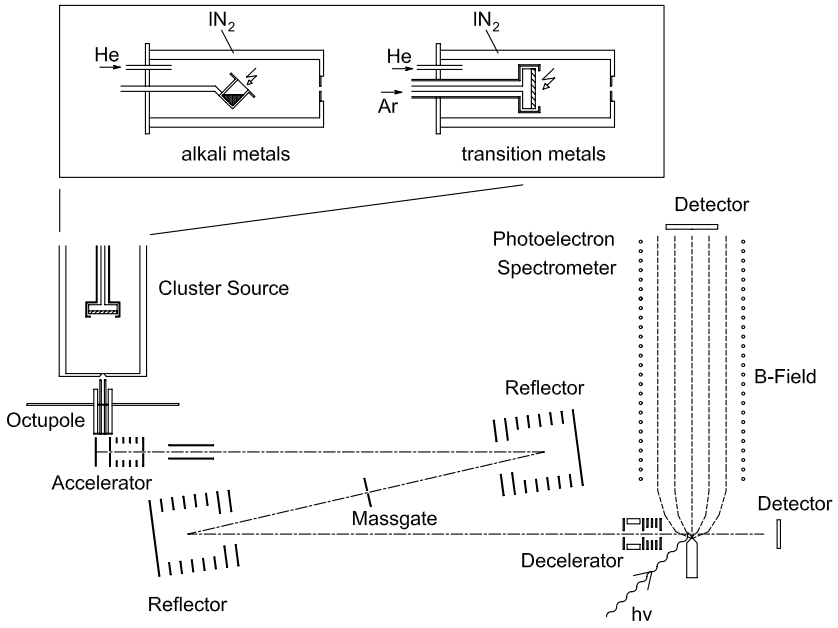

Figure 1. Schematic of the experimental setup. It consists of a cluster source, a thermalization radio frequency multipole ion trap, a high resolution tandem reflectron time-of-flight mass spectrometer, and a magnetic bottle type time-of-flight photoelectron spectrometer. Depending on the cluster materials in the cluster source either thermal evaporation or magnetron sputtering is applied to bring the material into the gas phase. See text for details.

2. Experiment

A schematic of the experiment is shown in Fig. 1. The clusters are produced in a gas aggregation source. Sodium is evaporated out of a crucible into a stream of helium with a pressure of about 0.5 mbar inside a liquid nitrogen cooled tube. In the helium the metal vapor condenses to clusters, the mean size of which can be controlled by parameters like the buffer gas pressure and flow velocity. A pulsed discharge at the end of the tube leads to charging of the clusters; roughly equal amounts of positively and negatively charged clusters are formed. The buffer gas with the clusters then expands through an adjustable iris aperture into the vacuum. The clusters enter an RF octupole, which guides them into the next chamber, where they are trapped and cooled in a liquid nitrogen cooled octupole trap (very recently this trap has been replaced by a 12 pole trap, which can be cooled by a cold head to temperatures of about 10 K). Bunches of cluster ions are extracted from the trap and inserted into a high resolution, double reflectron time-of-flight mass spectrometer, where a multiwire mass gate positioned at the focus point of the first reflector can be used to select clusters of a certain mass with a resolution of about m/dm=2000.

The size selected clusters get reflected (and rebunched) by the second reflector, are decelerated by a pulsed electric field and enter the interaction region of a magnetic bottle time-of-flight photoelectron spectrometer. Here the clusters are irradiated by a laser pulse; the magnetic field guides emitted electrons over a drift length of 1.6 m to a channeltron detector, where the flight time is measured. The flight time distributions obtained in this way are converted into kinetic energy distributions.

In order to obtain information about the character of the electron wavefunctions, recently an imaging photoelectron spectrometer[9] has been constructed. A drawing is shown in Fig. 2. The clusters enter the spectrometer on axis and are irradiated by a laser pulse. An inhomogeneous

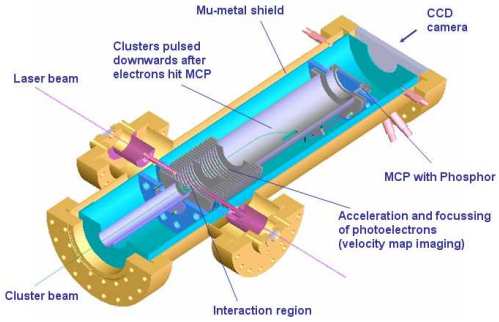

Figure 2. Imaging photoelectron spectrometer. The laser detached electrons are accelerated onto a multichannel plate and produce a spot pattern on its phosphor anode, which is recorded by a CCD camera. The inhomogeneous acceleration field follows the principle of velocity map imaging[8], which strongly reduces the influence of the finite ion-laser interaction volume onto the resolution of the spectrometer.

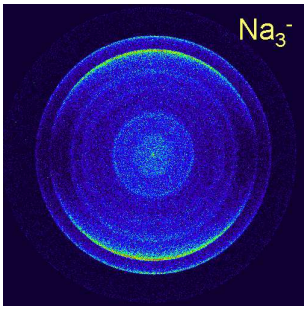

Figure 3. Imaging spectrum of Na_3^- recorded at a photon energy of 4.02 eV and vertical laser polarization (raw data). Electrons of different kinetic energy form circles of different radius; the angular distribution is directly visible. For quantitative evaluation this 2D projection of the electron velocities has to be transformed back into a 3D distribution [9].

electric field accelerates and focusses the emitted electrons onto a multichannelplate detector with phosphor screen anode (in velocity map imaging mode[8], which reduces the influence of the finite interaction volume). A CCD camera records the images on the phosphor screen, which are evaluated in real time in order to find the positions of the detected electrons. After the electrons have been detected by the MCP, the remaining clusters are pulsed downwards by applying a potential to the upper part of the drift tube in order to avoid wrong signals on the MCP. A typical image spectrum (measured on Na_3^- at a photon energy of 4.02 eV, vertical polarization) is shown in Fig. 3. One can see ring patterns, the radii of which indicate the velocities of the electrons. The angular distribution is directly visible. These images represent projections of the 3D velocity distributions of the electrons; for a quantitative analysis they have to be transformed back using Abel inversion or similar techniques[9, 10].

3. Energy resolved photoelectron spectroscopy

Examples of photoelectron spectra are shown in Fig. 4. These are the spectra of room temperature sodium cluster anions with 16 to 20 and 36 to 41 atoms. Na_{17}^- is a cluster with 18 valence electrons. In the free electron model its electronic configuration can be described as $1s^2\ 1p^6\ 1d^{10}$. Indeed in the photoelectron spectrum (PES) one can identify the big peak at about 1.8 eV binding energy as the 1d orbital, and the small peak at about 2.6 eV as the 1p orbital. An additional electron would have to fill the next higher shell, 2s. Indeed for Na_{18}^- one can see the appearance of a new peak. For Na_{19}^- this peak gets higher, as it is now filled with two electrons. Because only two electrons are allowed to occupy the 2s orbital, for the next size (Na_{20}^-) yet another shell appears, 1f. This shell then gets filled for the following sizes. At size 39 both this shell and the next higher 2p are filled. Adding an electron (by going to the next size, Na_{40}^-) leads to the appearance of the new 1g shell, which again grows in intensity for the following cluster sizes. Such shell filling patterns can be observed up to very large sizes [7, 11]. One example is shown in Fig. 5. Here the PES of Na_{309}^- is compared to its calculated density of states (DOS). Despite the large size of the cluster both the measured PES and the calculated

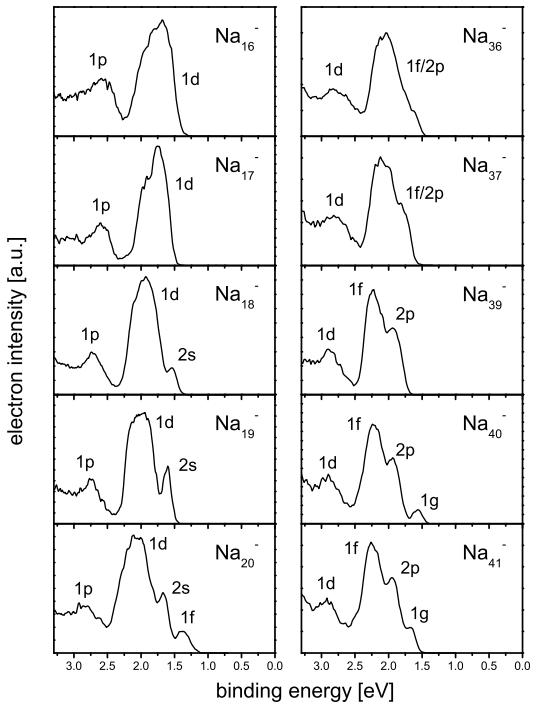

Figure 4. Photoelectron spectra of room temperature clusters Na_n^-, recorded at a photon energy of 4.02 eV. The visible bands are labeled by the quantum numbers of the corresponding states in the spherical free electron gas. Note the appearance of new shells for total valence electron numbers of 19, 21 and 41. [15]

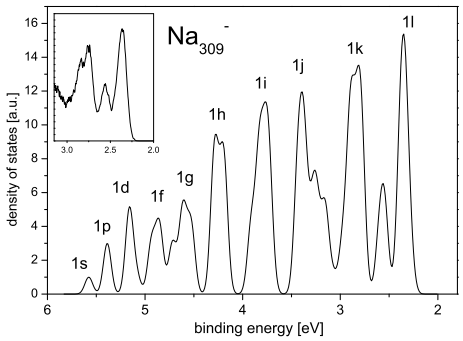

Figure 5. Electronic density of states of an icosahedral Na_{309}^-, calculated by DFT (calculations by M. Moseler[11]). Each Kohn-Sham-level is represented by a Gaussian with a width of 0.1 eV and a height of 0.5. The quantum numbers of the major shell sequence (with radial quantum number 1) are indicated. The inset shows the measured photoelectron spectrum of cold (∼100 K) Na_{309}^- recorded at a photon energy of 4.02 eV. Note the close to perfect agreement between the two distributions.

DOS are highly modulated. There is close to perfect agreement of the uppermost part of the calculated DOS with the measured PES (deeper lying states cannot be resolved in the PES as they are strongly broadened due to the very short lifetime of a hole in a deeper level). Obviously the DOS of a Na_{309}^- is highly discretized. One can tentatively assign angular momenta to the observed shells (only the values of the major sequence, that is for the lowest radial quantum number, are given). One has, however, to keep in mind that there is a non-negligible interaction between the electrons and ion lattice, which perturbs the angular momentum eigenstates[12]. In a real cluster angular momentum is not a good quantum number anymore. The reason why Na_{309}^- has such a simple DOS is that is has a high symmetry; it is a close packed 4 shell icosahedron [11]. Icosahedral symmetry allows for a high degeneracy of the electronic states; the angular momentum eigenstates split up into a well defined small number of sublevels [13, 14]. The question arises how much of the angular momentum eigenstate character is still preserved in the perturbed wavefunctions. One tool to test this is angle resolved PES, as will be discussed in the next section.

4. Angle resolved photoelectron spectroscopy

The angular distribution of electrons emitted in a single photon process out of an nonoriented molecule or cluster can be described by the following expression (in dipole approximation):

$$f(\theta) = 1 + \beta(\frac{3}{2}\cos^2\theta - \frac{1}{2}) \quad (1)$$

where θ is the angle with respect to the polarization direction of the light, and β is the anisotropy parameter, which can have values between -1 (emission perpendicular to the polarization) over 0 (isotropic emission) to 2 (emission parallel to the polarization). As has been shown already by Bethe[16] (for spherical single electron systems), this parameter strongly depends on the angular momentum of the initial state of the electron. One could therefore expect that different electronic shells in a cluster exhibit different angular distributions. One of the very first angle resolved spectra is presented in Fig. 6, which has been measured on a Na_{58}^- at a photon energy of 2.48 eV. In the top part a "normal" photoelectron is shown, as recorded with the magnetic bottle photoelectron spectrometer at a photon energy of 4.02 eV. Here one can recognize three electron shells: the largest peak (or band) can be identified as the completely filled 1g shell (the onset of which is visible in Fig. 4); the small peak at higher binding energy is the 2p shell, and the small peak at threshold is the 2d shell, which for this size is just filled with a single electron. The image beneath the spectrum shows the raw data as obtained from the imaging spectrometer, but in a cartesian plot of polar coordinates: the x-axis gives the radial position of a point on the multichannelplate detector, whereas the y-axis gives its angular position with respect to the vertical laser polarization. Although the radial position is proportional to the electron velocity and not its energy, the comparison nevertheless allows unambiguously to identify the three peaks described above in the angular distribution. It turns out that the three shells exhibit distinct differences; while the electron emission out of both the 2p and the 2d shell is peaked parallel to the laser polarization, the emission out of the 1g shell is perpendicular. Even more surprising is the uniformity of this behavior. Although the shells are clearly not fully degenerate (the 1g shell, e.g., is split into two bands, which seem to have some additional

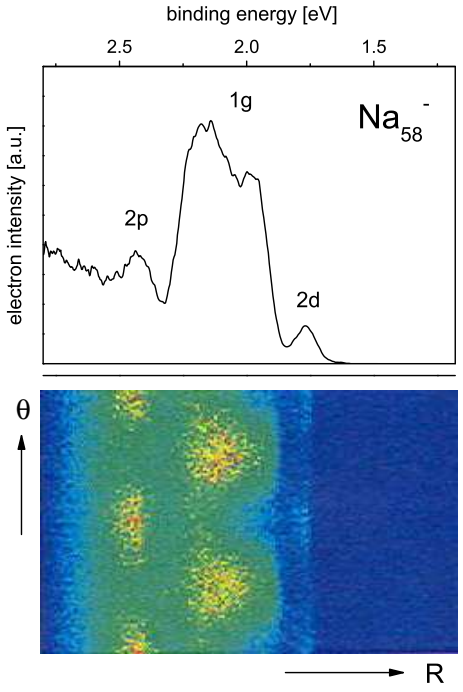

Figure 6. Angular distribution of photoelectrons. The upper panel shows the photoelectron spectrum of a Na_{58}^-, measured with the magnetic bottle electron spectrometer at a photon energy of 4.02 eV. The lower panel shows the raw data for the same cluster recorded with the imaging spectrometer at a photon energy of 2.48 eV. Positions on the detector are given by polar coordinates (R,θ), where R is the distance to the detector center, and θ is the angle with respect to the laser polarization. Note that electrons out of the 2p and the 2d shell are emitted preferentially in the direction of the laser polarization, whereas electrons out of the 1g shell are emitted perpendicularly.

substructure as well), all sublevels of one band exhibit very similar angular distributions. This demonstrates that the electron-lattice interaction is strong enough for lifting the degeneracy of the angular momentum eigenstates, but not for causing strong hybridization of the different angular momentum states, which would blur the differences between the shells. This is a very promising result, as it shows that the free electron model for sodium clusters is really justified, in the sense that the wavefunctions of the electrons in the clusters largely retain the character of truly free electron wavefunctions. This makes sodium clusters interesting model systems for the study of the dynamics of finite size Fermi systems. One example of such a study will be described in the next section.

5. Time resolved measurements

Due to the strong electron-electron and weak electron-ion interaction the electronic system of sodium clusters can be heated very efficiently by femtosecond laser pulses. This is most conveniently done at photon energies close to the strong collective plasmon resonance, which in sodium clusters is located at about 2.7 eV[4, 6, 17]. Here even at modest laser intensities of less than 10^{10} W/cm^2 several photons can be absorbed by a single cluster from a 100 fs pulse. The absorbed energy gets statistically distributed within the electron system on a very short timescale. The temperatures of the system reached in this process can get sufficiently high for thermal electron emission to occur[18]. This is demonstrated in Fig. 7; irradiation of a Na_{93}^+ cluster with femtosecond laser pulses of about 200 fs width and a photon energy of 3.1 eV leads to the emission of electrons with perfectly exponential energy distributions, as is typical for statistical thermal emission. Indeed the emission process can be very well modeled by statistical models like the Weisskopf model[18]. Changing the laser intensity (and thereby the number of photons absorbed) just leads to a change of the intensity of the emitted electrons and of the mean kinetic energy, that is the temperature of the electron gas.

This statistical emission process can be used to monitor the cooling of the electron gas by electron-phonon coupling in a pump-probe experiment[19]. Here two (cross-polarized) femtosecond laser pulses are used, the intensity of which is chosen such that a single laser pulse heats the cluster just up to about the onset of thermal electron emission. In this case the electron system is heated by the the first laser pulse without appreciable electron emission taking place. On a typical timescale of a few ps the electron system then cools by energy transfer to the vibrational modes of the lattice, that is by electron-phonon coupling. It gets reheated by the second laser pulse. If at this moment there is still some of the energy present absorbed from the first pulse, the temperature of the electron system will reach higher values, which causes a strong increase of the thermal electron emission. Measuring the total intensity of the emitted electrons therefore allows one to directly monitor the flow of energy out of the electron system. Examples of experimental results are shown in Fig. 8. Here the total electron intensity as a function of the delay time between the two laser pulses is shown for two cluster sizes, Na_{16}^+ and Na_{139}^+. The highest intensity is obtained for zero delay (when the highest temperatures of the electron gas are reached) and falls off approximately exponentially with increasing delay times. The curves are symmetrical with respect to time zero as (except for their polarization) identical laser pulses are used. Surprisingly the two quite different cluster sizes exhibit almost identical behavior; only a slightly faster decay can be observed for the smaller cluster (values of exponential fits are given). This demonstrates that at high temperatures even a highly discretized system like a Na_{16}^+ can exhibit purely statistical, bulk-like behavior, which is due to the very high density of excited states at such a degree of excitation. Such curves have been measured for a number of clusters. They have been evaluated using the simple two-temperature model, which assumes that both the electron and the phonon system can have different temperatures, and that the energy transfer between the two systems is proportional to the temperature difference [18]. The agreement between the simple model and the experiments was very good, which allowed to

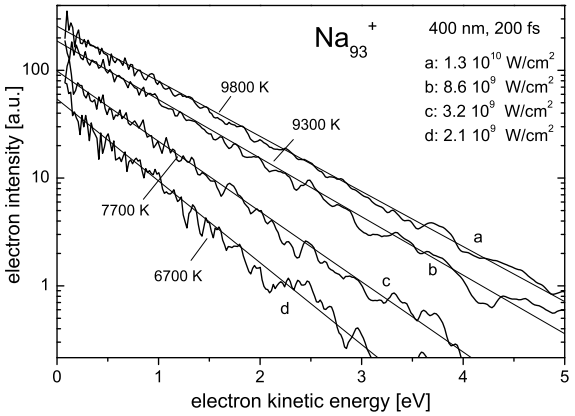

Figure 7. Kinetic energy distribution of electrons emitted from Na_{93}^+ clusters irradiated by single 200 fs, 400 nm laser pulses of different intensities. Purely exponential distributions are observed, which indicate thermal emission of electrons out of the strongly heated electron gas[18]. The corresponding temperatures of the electron gas as obtained from the slope of the curves are indicated.

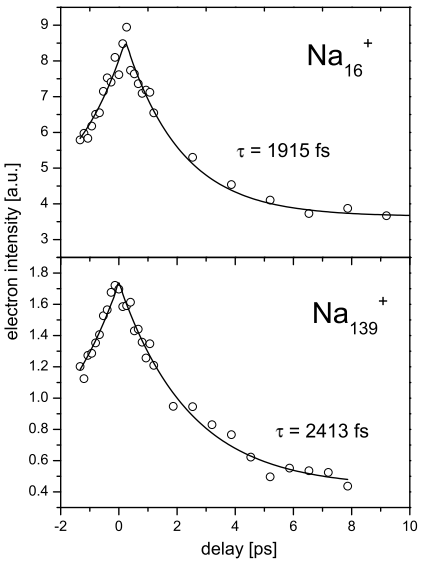

Figure 8. Pump-probe measurement of the electron gas cooling in free Na_n^+ clusters. The total intensity of thermally emitted electrons is measured as a function of the delay time between two identical laser pulses (400 nm, 200 fs, cross-polarized), which monitors the energy flow out of the electron system into the phonon system[19]. The observed long time constants of about 2 ps underline the weak electron-phonon coupling in sodium clusters.

extract reliable values of the electron phonon coupling strength. The main outcome, however, was the demonstration that, although these systems are highly excited and will fragment or even coulomb explode after a few nanoseconds, they are nevertheless at least in partial equilibrium and can be very well treated by statistical models.

6. Outlook: field amplification effects

One of the most fascinating aspects of the dynamics in simple metal clusters is the interplay between collective many particle excitations (namely the plasmon oscillation) and single particle excitations like electron emission. This interaction can be seen purely classical: the oscillating electron cloud produces a strong local electric field, which influences the kinetic energy of emitted electrons. In the case of strong excitation of the oscillation this can lead to very strong acceleration of the emitted electrons. Indeed such effects have been observed recently both in experiment and simulations[20]. Here the fields used were so strong that several tens of thousands of photons were absorbed by the cluster, which justifies a classical physics interpretation of the effects. The question arises how the field amplification will appear in the quantum regime, that is in cases where just a small number of photons are absorbed. The correct theoretical treatment of the coupling of a multiply excited plasmon to single particle excitations is still under discussion[21, 22]. The ideal experiment to test these theories is to excite a cold size-selected cluster with a narrow plasmon resonance by a fs laser pulse in resonance with the plasmon

and with a width comparable to the plasmon lifetime. From a measurement of energy and angle resolved photoelectron spectra as a function of the laser intensity (the number of photons absorbed) one should then be able to extract the magnitude of field amplification effects as well as more detailed information like the degree of anharmonicity of the plasmon excitation[21, 23]. Such experiments are underway.

7. Summary

Photoelectron spectroscopy on sodium clusters reveals a clear electron shell structure, which is most pronounced for clusters with a highly symmetric geometric structure. First results of angle resolved PES demonstrate the angular momentum eigenstate character of the electron shells. These properties, which are close to that of a finite free electron gas, make sodium clusters promising model systems for the study of multiparticle dynamics. Energy resolved PES in combination with fs-pump probe excitation already allowed a characterization of electron-phonon coupling in the clusters; it can be expected that angle resolved PES in combination with ultrashort laser excitation will allow to disentangle the various collective and single particle effects happening in the weak to medium strength excitation regime.

Acknowledgments

This work has been supported by the Deutsche Forschungsgemeinschaft. We thank Michael Moseler for providing the data shown in Fig. 5.

References

[1] Ashcroft NW, Mermin ND 1976 *Solid State Physics* (New York: Holt, Rinehart and Winston)
[2] Brack M 1993 *Rev. Mod. Phys.* **65** 677
[3] Knight WD, Clemenger K, deHeer WA, Saunders WA, Chou MY, Cohen ML 1984 *Phys. Rev. Lett.* **52** 2141
[4] de Heer WA 1993 *Rev. Mod. Phys.* **65** 611
[5] Haberland H, ed. 1995 *Clusters of Atoms and Molecules I* (Berlin: Springer-Verlag)
[6] Ekardt W, ed. 1999 *Metal Clusters* (Chichester: Wiley)
[7] Wrigge G, Astruc Hoffmann M, and v. Issendorff B. 2002 *Phys.Rev.* A **65** 063201
[8] Eppink ATJB, and Parker DH 1997 *Rev. Sci. Instrum.* **68** 3477
[9] Bordas C, Paulig F, Helm H and Huestis DL 1996 *Rev. Sci. Instrum.* **67** 2257
[10] Garcia GA , Nahon L, Powis I 2004 *Rev. Sci. Instrum.* **75** 4989
[11] Kostko O, Huber B, Moseler M, and v. Issendorff B 2007 *Phys. Rev. Lett.* **98** 043401
[12] Kostko O, Morgner N, Astruc Hoffmann M, and v.Issendorff B 2005 *Eur. Phys. J.* D **34** 133
[13] Häkkinen H, Moseler M, Kostko O, Morgner N, Astruc Hoffmann M, and v. Issendorff B 2004 *Phys. Rev. Lett.* **93** 093401
[14] Cheng HP, Berry RS, and Whetten RL 1991 *Phys. Rev.* B **43** 10470
[15] Moseler M, Huber B, Häkkinen H, Landman U, Wrigge G, Astruc Hoffmann M, and v. Issendorff B 2003 *Phys. Rev.* B **68** 165413
[16] Bethe H 1933 *Handbuch der Physik* **24** (Berlin: Springer)
[17] Schmidt M and Haberland H 2001 *Eur.Phys.J.* D **6** 109
[18] Schlipper R, Kusche R, v.Issendorff B and Haberland H 2001 *App.Phys.* A. **72** 255
[19] Maier M, Wrigge G, Astruc Hoffmann M, Didier P, and v. Issendorff B 2006 *Phys. Rev. Lett.* **96** 117405
[20] Fennel T, Döppner T, Passig J, Schaal C, Tiggesbäumker J, and Meiwes-Broer KH 2007 *Phys. Rev. Lett.* **98** 143401
[21] Gerchikov LG, Guet C, and Ipatov AN 2002 *Phys. Rev.* A **66** 053202
[22] Calvayrac F, Reinhard PG, Suraud E, and Ullrich CA 2000 *Phys. Rep.* **337** 493
[23] Catara F, Chomaz Ph, Van Giai N 1993 *Phys. Rev.* B **48** 18207